5LMA0 – Project heat diffusion

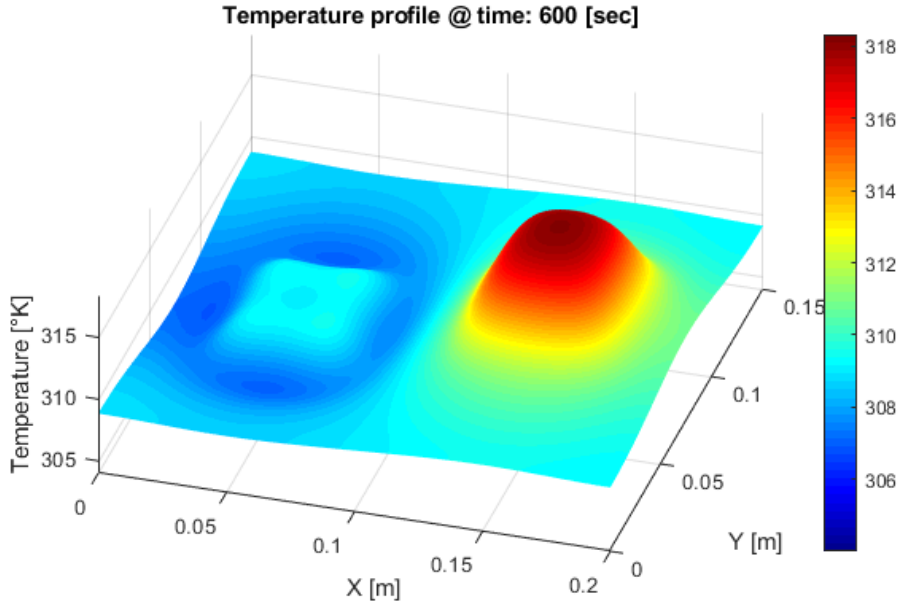

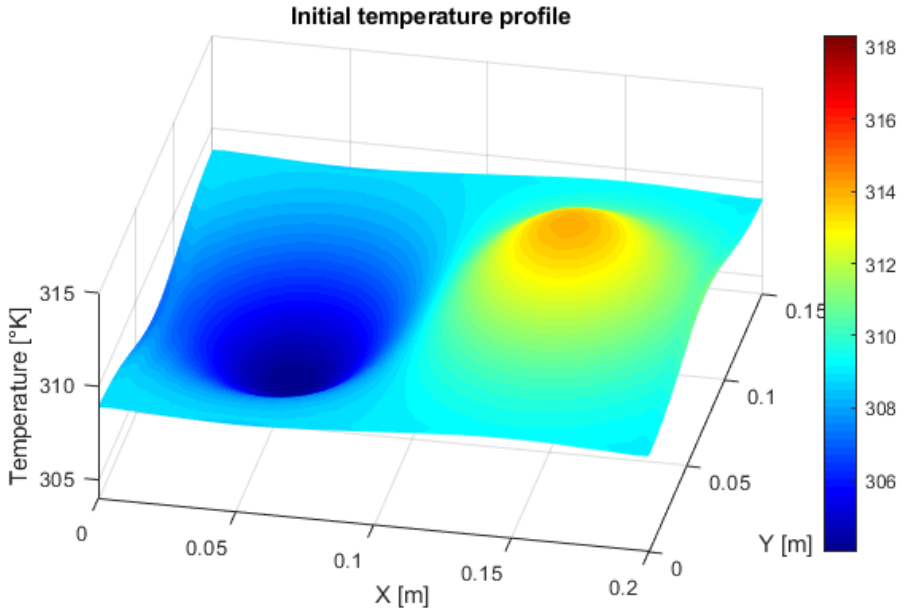

Date:
3 February 2019

Names:	**Student number:**
Bob Clephas	1271431
Job Meijer	1268155

Table of contents

Introduction

In this project a model for hyperthermia is considered which describes how a temperature distribution on a locally heated surface evolves over time. A rectangular area is considered of dimension $L_x \times L_y$ as shown in Figure 1. Here the green areas $u1$ and $u2$ are defined as inputs where the heat fluxes are applied, the yellow area is normal tissue and the orange area is tumor tissue with dimensions $\ell_x \times \ell_y$.

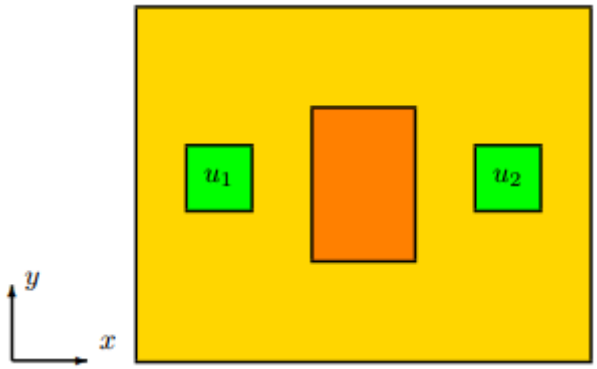

Figure 1 – Configuration of surface with heat flux locations

The model is described by the following parabolic partial differential equation:

$$\rho(x,y)c(x,y)\frac{\delta T}{\delta t}(x,y,t) = \begin{bmatrix}\frac{\delta}{\delta x} & \frac{\delta}{\delta y}\end{bmatrix} K(x,y) \begin{bmatrix}\frac{\delta T(x,y)}{\delta x} \\ \frac{\delta T(x,y)}{\delta y}\end{bmatrix} + u(x,y,t)$$

where

Symbol	Description	Unit	Value
L_x	Length	[m]	0.2
L_y	Width	[m]	0.15
ρ	Material densities (yellow, orange area)	[kg/m^3]	1100, 1000
c	Heat capacities (yellow, orange area)	[J/(kg K)]	3890, 3350
κ	Thermal conductivities (yellow, orange area)	[W/(m K)]	0.31, 0.31
(X_1,Y_1)	Location heat flux 1	([m],[m])	(L_x/4, L_y/2)
(X_2,Y_2)	Location heat flux 2	([m],[m])	(3L_x/4, L_y/2)
W	Actuator width	[m]	0.05
$T_{ambient}$	Ambient temperature	[K]	309

Table 1 – Model properties

Furthermore, the output of the model is the temperature of the surface in degrees Kelvin defined by $T_{ambient} + T(x,y,t)$.

The purpose of this project is to derive a fast and simple model that accurately describes the temperature evolution of this system, as explained in the following ten exercises.

Exercise 1

In this exercise is proven whether the system is linear or nonlinear and whether the system is time-variant or time-invariant. While doing so, the two cases where the model is homogeneous or non-homogeneous are distinguished.

If the model is **homogeneous** (1), ρ, c and K do not depend on the position (x, y). The system is linear, because a summation of inputs results in a summation of their respective outputs (2). The system is time-invariant because the output does not change when a time shifted input is applied (3).

$$\rho c \frac{\delta T}{\delta t}(x, y, t) = \kappa \left(\frac{\delta^2 T(x, y, t)}{\delta x^2} + \frac{\delta^2 T(x, y, t)}{\delta y^2} \right) + u(x, y, t) \tag{1}$$

$$\rho c \frac{\delta (T_1 + T_2)}{\delta t} = \kappa \left(\frac{\delta^2 (T_1 + T_2)}{\delta x^2} + \frac{\delta^2 (T_1 + T_2)}{\delta y^2} \right) + (u_1 + u_2) \tag{2}$$

$$\rho c \frac{\delta T}{\delta t}(x, y, t + \tau) = \kappa \left(\frac{\delta^2 T(x, y, t + \tau)}{\delta x^2} + \frac{\delta^2 T(x, y, t + \tau)}{\delta y^2} \right) + u(x, y, t + \tau) \tag{3}$$

When the model is **non-homogeneous** (4), ρ, c and K do depend on the position (x, y). The system is still linear, because a summation of inputs still results in a summation of their respective outputs (5). The non-homogeneous system is also still time-invariant because the output does not change when a time shifted input is applied (6).

$$\rho(x, y) c(x, y) \frac{\delta T}{\delta t}(x, y, t) = \kappa \left(\frac{\delta^2 T(x, y)}{\delta x^2} + \frac{\delta^2 T(x, y)}{\delta y^2} \right) + u(x, y, t) \tag{4}$$

$$\rho(x, y) c(x, y) \frac{\delta (T_1 + T_2)}{\delta t} = \kappa \left(\frac{\delta^2 (T_1 + T_2)}{\delta x^2} + \frac{\delta^2 (T_1 + T_2)}{\delta y^2} \right) + (u_1 + u_2) \tag{5}$$

$$\rho(x, y) c(x, y) \frac{\delta T}{\delta t}(x, y, t + \tau) = \kappa \left(\frac{\delta^2 T(x, y, t + \tau)}{\delta x^2} + \frac{\delta^2 T(x, y, t + \tau)}{\delta y^2} \right) + u(x, y, t + \tau) \tag{6}$$

Exercise 2

For now, it is assumed that the model is homogeneous and isotropic, meaning that $\ell_x = \ell_y = 0$ (no orange area) and $\rho(x, y) = \rho, c(x, y) = c$ and $K(x, y) = \kappa$ are positive constants.

In this exercise it is shown that the system admits to the form $T(x, y, t) = a(t)\phi^{(x)}\phi^{(y)}$ whenever $u(x, y, t) = 0$. Here $a, \phi^{(x)}$ and $\phi^{(y)}$ are scalar-valued functions on $\mathbb{R}$, $[0, L_x]$ and $[0, L_y]$, respectively, that satisfy the separated differential equations (7) for suitable constants λ_x, λ_y and λ.

$$\ddot{\phi}^{(x)} - \lambda_x \phi^{(x)} = 0, \quad \ddot{\phi}^{(y)} - \lambda_y \phi^{(y)} = 0, \quad \dot{a} - \lambda_a a = 0 \tag{7}$$

When $u(x, y, t) = 0$, this results in the following equation:

$$\frac{\delta T}{\delta t} = \frac{\kappa}{\rho c} \left(\frac{\delta^2 T}{\delta x^2} + \frac{\delta^2 T}{\delta y^2} \right) \tag{8}$$

Now $T(x, y, t)$ is substituted by $a(t)\phi^{(x)}\phi^{(y)}$, resulting in the following equation:

$$\dot{a}\phi^{(x)}\phi^{(y)} = \frac{\kappa}{\rho c} \left(\ddot{\phi}^{(x)} a \phi^{(y)} + \ddot{\phi}^{(y)} a \phi^{(x)} \right) \tag{9}$$

This can be rewritten in the following three equations:

$$\ddot{\phi}^{(x)} - \left(\frac{\rho c}{\kappa a}\dot{a} - \frac{\ddot{\phi}^{(y)}}{\phi^{(y)}}\right)\phi^{(x)} = 0, \quad \ddot{\phi}^{(y)} - \left(\frac{\rho c}{\kappa a}\dot{a} - \frac{\ddot{\phi}^{(x)}}{\phi^{(x)}}\right)\phi^{(y)} = 0, \quad \dot{a} - \frac{\kappa}{\rho c}\left(\frac{\ddot{\phi}^{(x)}}{\phi^{(x)}} + \frac{\ddot{\phi}^{(y)}}{\phi^{(y)}}\right)a = 0 \qquad (10)$$

Now the following lambdas are defined:

$$\lambda_x = \frac{\ddot{\phi}^{(x)}}{\phi^{(x)}}, \qquad \lambda_y = \frac{\ddot{\phi}^{(y)}}{\phi^{(y)}}, \qquad \lambda_a = \frac{\dot{a}}{a} \qquad (11)$$

Using these lambdas results in the following equations:

$$\ddot{\phi}^{(x)} - \left(\frac{\rho c}{\kappa}\lambda_a - \lambda_y\right)\phi^{(x)} = 0, \qquad \ddot{\phi}^{(y)} - \left(\frac{\rho c}{\kappa}\lambda_a - \lambda_x\right)\phi^{(y)} = 0, \qquad \dot{a} - \frac{\kappa}{\rho c}(\lambda_x + \lambda_y)a = 0 \qquad (12)$$

These can be substituted which results in:

$$\frac{\rho c}{\kappa}\lambda_a - \lambda_y = \lambda_x, \qquad \frac{\rho c}{\kappa}\lambda_a - \lambda_x = \lambda_y, \qquad \frac{\kappa}{\rho c}(\lambda_x + \lambda_y) = \lambda_a \qquad (13)$$

These lambdas are the initial conditions of the simplified model.

Exercise 3

In this exercise is shown that for any $K > 0$ and $L > 0$ the set $\{\phi_{k,l} \,|0 \le k \le K, 0 \le \ell \le L\}$ is an orthonormal set of functions in L_2.

First the functions for $\phi_k^{(x)}(x)$ and $\phi_\ell^{(y)}(y)$ are defined:

$$\phi_k^{(x)}(x) = \begin{cases} \frac{1}{\sqrt{L_x}} \; if \; k = 0 \\ \sqrt{\frac{2}{L_x}}\cos\left(\frac{k\pi x}{L_x}\right) if \; k > 0 \end{cases} \qquad \phi_\ell^{(y)}(y) = \begin{cases} \frac{1}{\sqrt{L_y}} \; if \; \ell = 0 \\ \sqrt{\frac{2}{L_y}}\cos\left(\frac{\ell\pi y}{L_y}\right) \; if \; \ell > 0 \end{cases} \qquad (14)$$

These functions can be combined into $\phi_{k,\ell}(x, y)$, as can be seen below.

$$\phi_{k,\ell}(x, y) = \phi_k^{(x)}(x)\phi_\ell^{(y)}(y) \qquad (15)$$

Now the inner product space L_2, based on $\phi_{k,\ell}(x, y)$, is computed:

$$\langle \phi_i, \phi_j \rangle = \int_0^{L_x}\int_0^{L_y} \phi_i(x, y)\phi_j(x, y)dydx \qquad (16)$$

To proof that $\phi_{k,\ell}$ is an orthonormal set of functions in L_2 the following statement has to hold:

$$\langle \phi_i, \phi_j \rangle = \begin{cases} 1 \; if \; i = j \\ 0 \; if \; i \neq j \end{cases} \qquad (17)$$

The following is defined for any $K > 0$ and $L > 0$ and $0 \le k \le K, 0 \le \ell \le L$:

$$k_i = i \; mod \; K, \qquad \ell_i = \left\lfloor \frac{i}{K} \right\rfloor \qquad (18)$$

The next step is to define $\phi_i(x,y)$, which is done for different conditions based on k_i and ℓ_i:

$$\phi_i(x,y) = \begin{cases} \frac{1}{\sqrt{L_x L_y}} \; if \; k_i = \ell_i = 0 \\ \sqrt{\frac{2}{L_x L_y}} \cos\left(\frac{\ell_i \pi y}{L_y}\right) \; if \; k_i = 0 \; and \; \ell_i > 0 \\ \sqrt{\frac{2}{L_x L_y}} \cos\left(\frac{k_i \pi x}{L_x}\right) \; if \; k_i > 0 \; and \; \ell_i = 0 \\ \frac{2}{\sqrt{L_x L_y}} \cos\left(\frac{k_i \pi x}{L_x}\right) \cos\left(\frac{\ell_i \pi y}{L_y}\right) \; if \; k_i > 0 \; and \; \ell_i > 0 \end{cases} \tag{19}$$

When computing the inner product (16) the outcome is 1 if $i = j$ and 0 when $i \neq j$, leading to the conclusion that the set $\{\phi_{k,l} \,|0 \leq k \leq K, 0 \leq \ell \leq L\}$ is an orthonormal set of functions in L_2 for any $K > 0$ and $L > 0$.

Exercise 4

To be able to simulate the model, The Galerkin projection is used to transform the homogeneous and isotropic form of the model (1) into an ordinary differential equation. Using the spectral decomposition of the temperature evolution (20) and the definition for the combined spectral components (15), the spectra decomposition of the temperature evolution (21) is defined.

$$T(x,y,t) = \sum_{k=0}^{\infty} \sum_{l=0}^{\infty} a_{k,l}(t) \phi_k^{(x)}(x) \phi_l^{(y)}(y) \tag{20}$$

$$T(x,y,t) = \sum_{k=0}^{\infty} \sum_{l=0}^{\infty} a_{k,l}(t) \phi_{k,l}(x,y) \tag{21}$$

Replacing the double indexing k, l with i results in the spectral decomposition of the temperature evolution (22).

$$T(x,y,t) = \sum_{i=0}^{\infty} a_i(t) \phi_i(x,y) \tag{22}$$

To calculate the Galerkin projection, the inner product of the model and the defined basis function ϕ_j is calculated using a standard inner product as defined in (16) which results in equation (23).

$$\langle \rho c \frac{\delta T}{\delta t}, \phi_j \rangle = \langle \kappa \left(\frac{\delta^2 T}{\delta x^2} + \frac{\delta^2 T}{\delta y^2} \right) + u, \phi_j \rangle \tag{23}$$

Substituting the spectral decomposition of the temperature evolution results in equation (24)

$$\langle \rho c \sum_{i=0}^{\infty} \dot{a}_i \phi_i \, , \phi_j \rangle = \langle \kappa \left(\sum_{i=0}^{\infty} a_i \ddot{\phi}_i^{(x)} + \sum_{i=0}^{\infty} a_i \ddot{\phi}_i^{(y)} \right) + u, \phi_j \rangle \tag{24}$$

Because the defined inner product (16) is a linear operator, the equation can be rewritten into equation (25) and subsequently equation (26). From the definition it can also be seen that everything that is not a function of x or y can be treated as a constant which results in equation (27).

$$\langle \rho c \sum_{i=0}^{\infty} \dot{a}_i \phi_i , \phi_j \rangle = \langle \kappa \sum_{i=0}^{\infty} a_i \ddot{\phi}_i^{(x)} , \phi_j \rangle + \langle \kappa \sum_{i=0}^{\infty} a_i \ddot{\phi}_i^{(y)} , \phi_j \rangle + \langle u, \phi_j \rangle \tag{25}$$

$$\sum_{i=0}^{\infty} \langle \rho c \dot{a}_i \phi_i, \phi_j \rangle = \sum_{i=0}^{\infty} \langle \kappa a_i \ddot{\phi}_i^{(x)}, \phi_j \rangle + \sum_{i=0}^{\infty} \langle \kappa a_i \ddot{\phi}_i^{(y)}, \phi_j \rangle + \langle u, \phi_j \rangle \tag{26}$$

$$\sum_{i=0}^{\infty} \rho c \dot{a}_i \langle \phi_i, \phi_j \rangle = \sum_{i=0}^{\infty} \kappa a_i \left(\langle \ddot{\phi}_i^{(x)}, \phi_j \rangle + \langle \ddot{\phi}_i^{(y)}, \phi_j \rangle \right) + \langle u, \phi_j \rangle \tag{27}$$

Due to the orthonormality of the basis function the equation can be rewritten into equation (28).

$$\sum_{i=0}^{\infty} \rho c \dot{a}_i = \sum_{i=0}^{\infty} \kappa a_i \left(\langle \ddot{\phi}_i^{(x)}, \phi_j \rangle + \langle \ddot{\phi}_i^{(y)}, \phi_j \rangle \right) + \langle u, \phi_j \rangle \tag{28}$$

Rewriting this into matrix form for $j \in \mathbb{N}$ gives an ordinary differential equation (29).

$$\begin{bmatrix} \dot{a}_0 \\ \vdots \\ a_i \\ \vdots \\ \dot{a}_\infty \end{bmatrix} = \frac{\kappa}{\rho c} \begin{bmatrix} \langle \ddot{\phi}_0^{(x)}, \phi_0 \rangle + \langle \ddot{\phi}_0^{(y)}, \phi_0 \rangle & \dots & \langle \ddot{\phi}_i^{(x)}, \phi_0 \rangle + \langle \ddot{\phi}_i^{(y)}, \phi_0 \rangle & \dots & \langle \ddot{\phi}_\infty^{(x)}, \phi_0 \rangle + \langle \ddot{\phi}_\infty^{(y)}, \phi_0 \rangle \\ \vdots & \ddots & \vdots & \ddots & \vdots \\ \langle \ddot{\phi}_0^{(x)}, \phi_j \rangle + \langle \ddot{\phi}_0^{(y)}, \phi_j \rangle & \dots & \langle \ddot{\phi}_i^{(x)}, \phi_j \rangle + \langle \ddot{\phi}_i^{(y)}, \phi_j \rangle & \dots & \langle \ddot{\phi}_\infty^{(x)}, \phi_j \rangle + \langle \ddot{\phi}_\infty^{(y)}, \phi_j \rangle \\ \vdots & \ddots & \vdots & \ddots & \vdots \\ \langle \ddot{\phi}_0^{(x)}, \phi_\infty \rangle + \langle \ddot{\phi}_0^{(y)}, \phi_\infty \rangle & \dots & \langle \ddot{\phi}_i^{(x)}, \phi_\infty \rangle + \langle \ddot{\phi}_i^{(y)}, \phi_\infty \rangle & \dots & \langle \ddot{\phi}_\infty^{(x)}, \phi_\infty \rangle + \langle \ddot{\phi}_\infty^{(y)}, \phi_\infty \rangle \end{bmatrix} \begin{bmatrix} a_0 \\ \vdots \\ a_i \\ \vdots \\ a_\infty \end{bmatrix} + \frac{1}{\rho c} \begin{bmatrix} \langle u, \phi_0 \rangle \\ \vdots \\ \langle u, \phi_j \rangle \\ \vdots \\ \langle u, \phi_\infty \rangle \end{bmatrix} \tag{29}$$

Substituting the basis functions results in equation (30).

$$\begin{bmatrix} \dot{a}_0 \\ \vdots \\ a_i \\ \vdots \\ \dot{a}_\infty \end{bmatrix} = \frac{\kappa}{\rho c} \begin{bmatrix} 0 & \dots & 0 & \dots & 0 \\ \vdots & \ddots & \vdots & \ddots & \vdots \\ 0 & \dots & -\left(\left(\frac{k_i \pi}{Lx} \right)^2 + \left(\frac{l_i \pi}{Ly} \right)^2 \right) & \dots & 0 \\ \vdots & \ddots & \vdots & \ddots & \vdots \\ 0 & \dots & 0 & \dots & -\left(\left(\frac{\infty \pi}{Lx} \right)^2 \left(\frac{\infty \pi}{Ly} \right)^2 \right) \end{bmatrix} \begin{bmatrix} a_0 \\ \vdots \\ a_i \\ \vdots \\ a_\infty \end{bmatrix} + \frac{1}{\rho c} \begin{bmatrix} \langle u, \phi_0 \rangle \\ \vdots \\ \langle u, \phi_j \rangle \\ \vdots \\ \langle u, \phi_\infty \rangle \end{bmatrix} \tag{30}$$

To derive the equilibrium solution of the model, the input is set to 0, leading to equation (31).

$$\begin{bmatrix} \dot{a}_0 \\ \vdots \\ a_i \\ \vdots \\ \dot{a}_\infty \end{bmatrix} = \frac{\kappa}{\rho c} \begin{bmatrix} 0 & \dots & 0 & \dots & 0 \\ \vdots & \ddots & \vdots & \ddots & \vdots \\ 0 & \dots & -\left(\left(\frac{k_i \pi}{Lx} \right)^2 + \left(\frac{l_i \pi}{Ly} \right)^2 \right) & \dots & 0 \\ \vdots & \ddots & \vdots & \ddots & \vdots \\ 0 & \dots & 0 & \dots & -\left(\left(\frac{\infty \pi}{Lx} \right)^2 \left(\frac{\infty \pi}{Ly} \right)^2 \right) \end{bmatrix} \begin{bmatrix} a_0 \\ \vdots \\ a_i \\ \vdots \\ a_\infty \end{bmatrix} \tag{31}$$

The free response of the model, which is in the form $\dot{a} = Aa$, can be calculated using equation (32) resulting in equation (33).

$$a(t) = e^{At} a(0) \tag{32}$$

$$a(t) = \begin{bmatrix} e^0 & \dots & 0 & \dots & 0 \\ \vdots & \ddots & \vdots & \ddots & \vdots \\ 0 & \dots & e^{-\frac{\kappa}{\rho c}\left(\left(\frac{k_i \pi}{Lx} \right)^2 + \left(\frac{l_i \pi}{Ly} \right)^2 \right) t} & \dots & 0 \\ \vdots & \ddots & \vdots & \ddots & \vdots \\ 0 & \dots & 0 & \dots & e^{-\frac{\kappa}{\rho c}\left(\left(\frac{\infty \pi}{Lx} \right)^2 \left(\frac{\infty \pi}{Ly} \right)^2 \right) t} \end{bmatrix} a(0) \tag{33}$$

The equilibrium solution can be obtained by equating the solution at $t = \infty$, which results in the a coefficients as can be seen in (34).

$$a(\infty) = \begin{bmatrix} a_0(0) \\ 0 \\ \vdots \\ 0 \end{bmatrix} \tag{34}$$

Filling in the coefficients (34) in equation (22) gives the equilibrium solution (35) of the model. Substituting the basis function ϕ_0 and replacing $a_0(0)$ with the inner product of Initial temperature for the model and the basis function results in equation (36). Which is as expected the average temperature of the initial temperature profile.

$$T(x, y, \infty) = a_0(0)\phi_0(x, y) \tag{35}$$

$$T(x, y, \infty) = \frac{1}{LxLy} \int_0^{L_x} \int_0^{L_y} T(x, y, 0) dy dx \tag{36}$$

Exercise 5

During this exercise the model is simulated using model parameters of Table 1 and no input heat fluxes. The initial temperature profile is a 2D Bell curve with height +5 [°K] and a width of 0.02 [m]. The simulation is executed with $K = L = 3, 5, 10, 20$ as shown in Figure 2, Figure 3, Figure 4 and Figure 5.

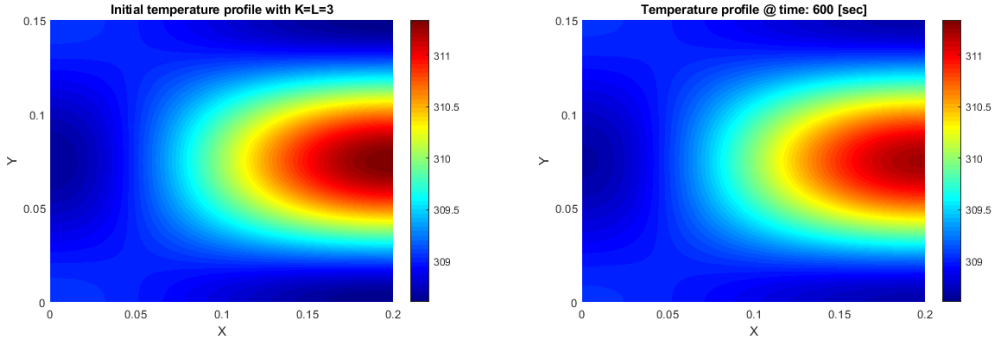

Figure 2 – Initial temperature profile over time with K=L=3

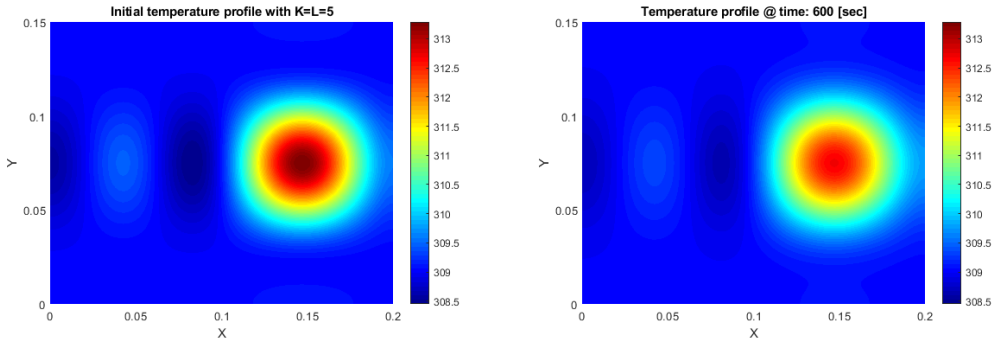

Figure 3 – Initial temperature profile over time with K=L=5

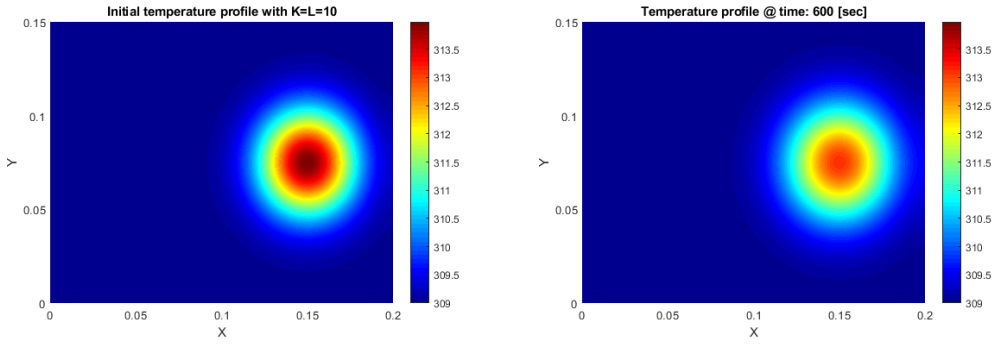

Figure 4 – Initial temperature profile over time with K=L=10

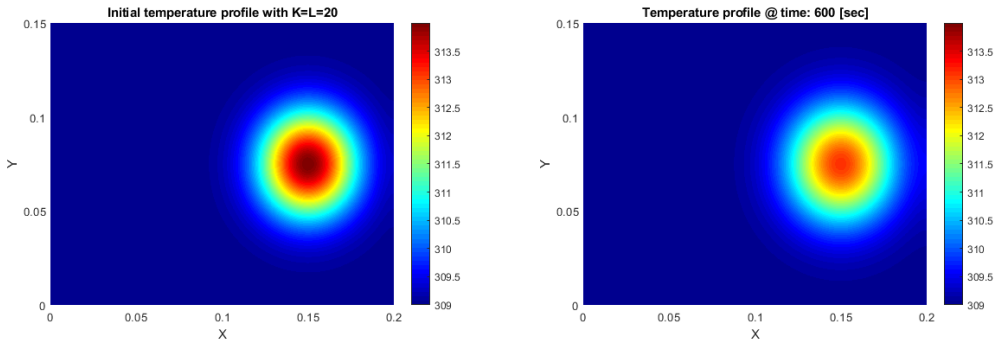

Figure 5 – Initial temperature profile over time with K=L=20

Exercise 6

During this exercise the simulation is executed with

- Different initial temperature profiles
- Inputs for the heat fluxes $u_1(t)$ and $u_2(t)$

while varying with the approximation orders K and L.

The initial temperature profile is now changed to two 2D Bell curves at the location of $u_1(t)$ and $u_2(t)$ and a radius of 0.03 [m]. The Bell curve at the location of $u_1(t)$ has an initial peak temperature of +5 [°K] and the Bell curve at location $u_2(t)$ has an initial peak temperature of -5 [°K]. This initial profile is simulated with the same approximation orders of exercise 5. The results of these simulations are shown in Figure 6, Figure 7, Figure 8 and Figure 9.

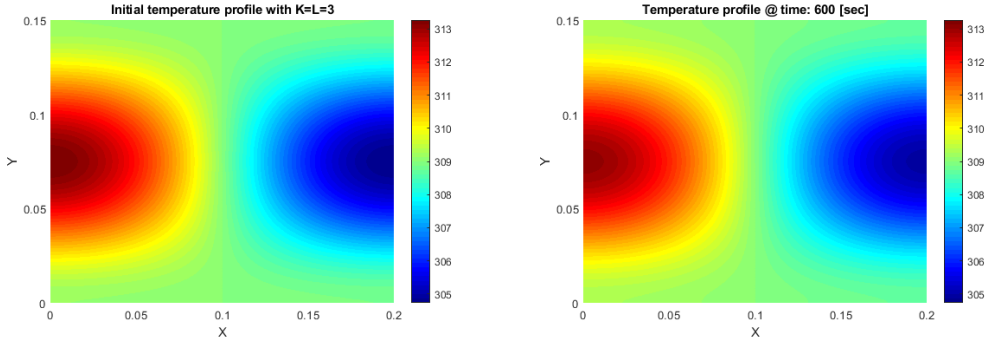

Figure 6 – Double Bell curve initial profile with K=L=3

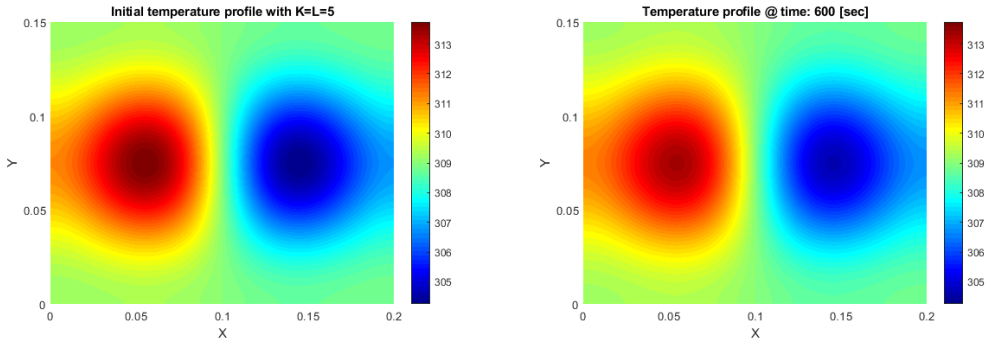

Figure 7 – Double Bell curve initial profile with K=L=5

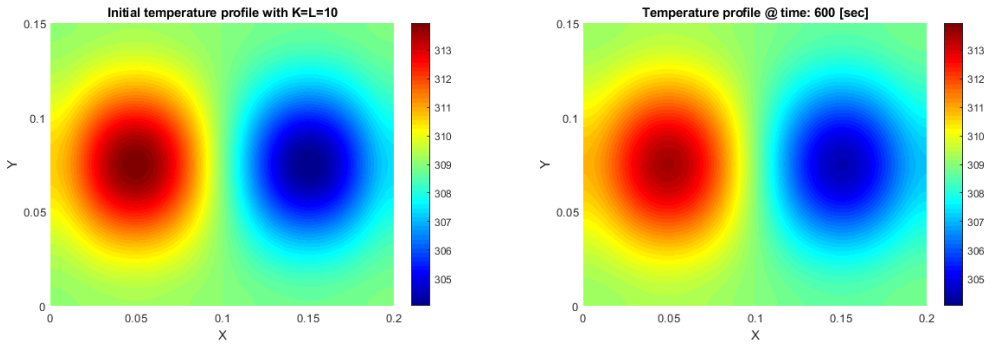

Figure 8 – Double Bell curve initial profile with K=L=10

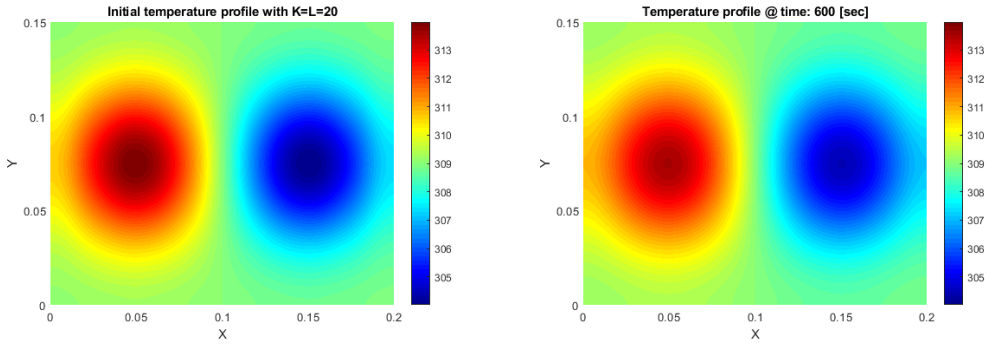

Figure 9 – Double Bell curve initial profile with K=L=20

Now the inputs $u_1(t)$ and $u_2(t)$ are added to the simulation with the following properties:

- Start at t=30
- Stop at t=330
- Heat flux = 60,000

and with the same initial temperature profile and values for K and L as in exercise 5, resulting in Figure 10, Figure 11, Figure 12 and Figure 13.

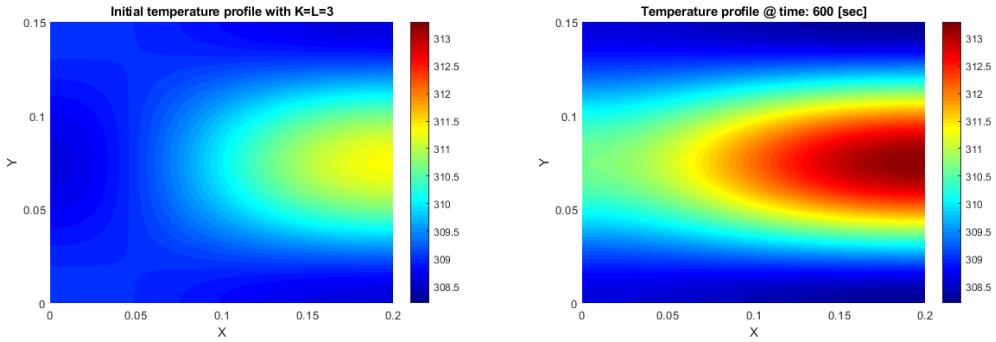

Figure 10 – Initial temperature profile with inputs u1 and u2 over time with K=L=3

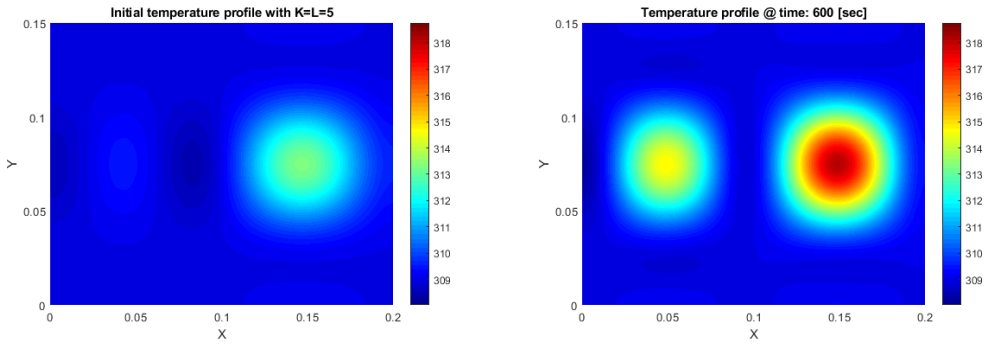

Figure 11 – Initial temperature profile with inputs u1 and u2 over time with K=L=5

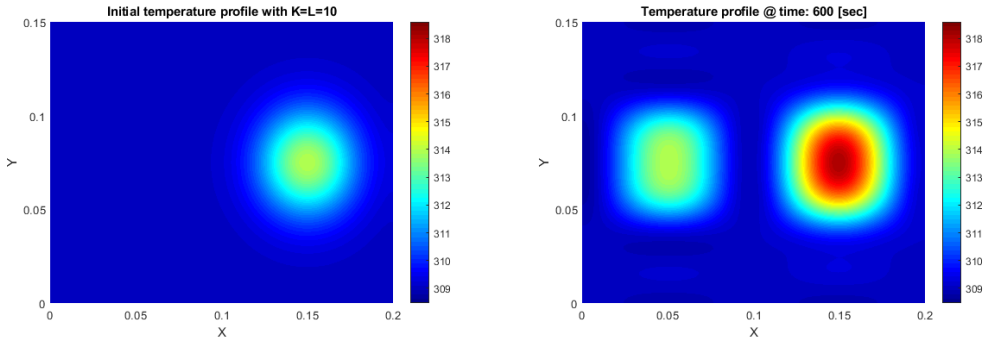

Figure 12 – Initial temperature profile with inputs u1 and u2 over time with K=L=10

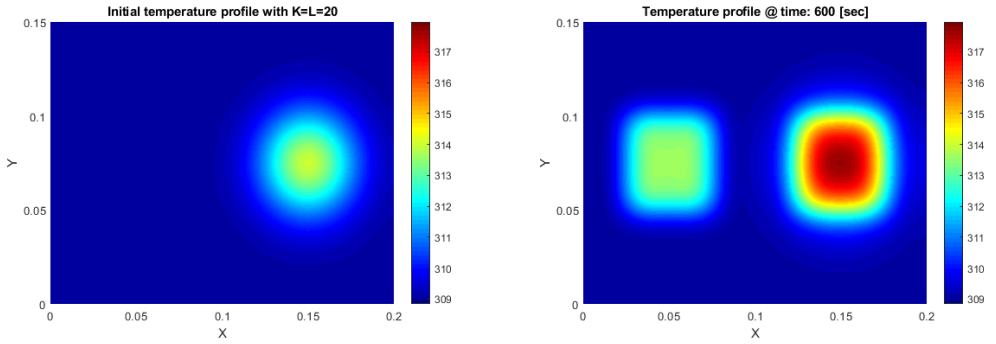

Figure 13 – Initial temperature profile with inputs u1 and u2 over time with K=L=20

From these simulations can be concluded that with higher approximation orders for K and L the results are more accurate. If the approximation order is low, harmonics are visible in the temperature profile. With an approximation order of 3 or lower the result is inaccurate.

Exercise 7

In this exercise the output of the simulation is taken with a high approximation order $K = L = 50$ and this data is used to compute a POD basis $\{\phi_i\}_{i=1,\dots,R}$ in L_2 of order R. The POD basis is created using the (economy-size) Singular Value Decomposition (SVD) of the high order approximation data $T(x, y, t)$ as shown in (37). The basis is now defined by the columns of U, $U = (\phi_1, \dots, \phi_R)$

$$[U, S, Y] = svd(T(x, y, t), 'econ') \tag{37}$$

Exercise 8

Now the POD basis ϕ_i from exercise 7 is used to create a reduced order POD model that takes the heat fluxes $u_1(t)$ and $u_2(t)$ as inputs and outputs the coefficients $a_i(t)$ in the truncated expansion:

$$T_R(x, y, t) = \sum_{i=1}^{R} a_i(t)\phi_i(x, y) \tag{38}$$

Exercise 9

The next step is to validate the quality of the reduced order POD model from exercise 8 by simulating with different orders of R, different initial temperature profiles and different heat fluxes $u_1(t)$ and $u_2(t)$. To compare the POD basis to the earlier determined basis, the same orders for R are used as for K and L.

First the reduced order POD model is simulated with the same initial temperature profile as during exercise 5 with varying $R = 3{,}20$ as shown in Figure 14 and Figure 15 which are almost identical figures.

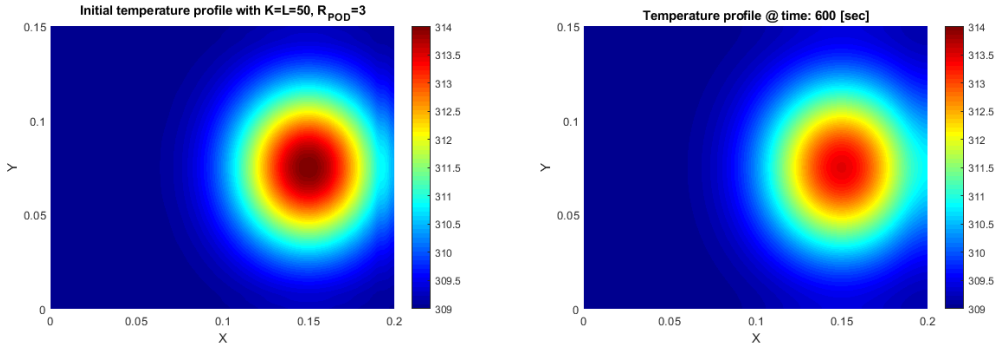

Figure 14 – POD basis initial profile over time with order R=3

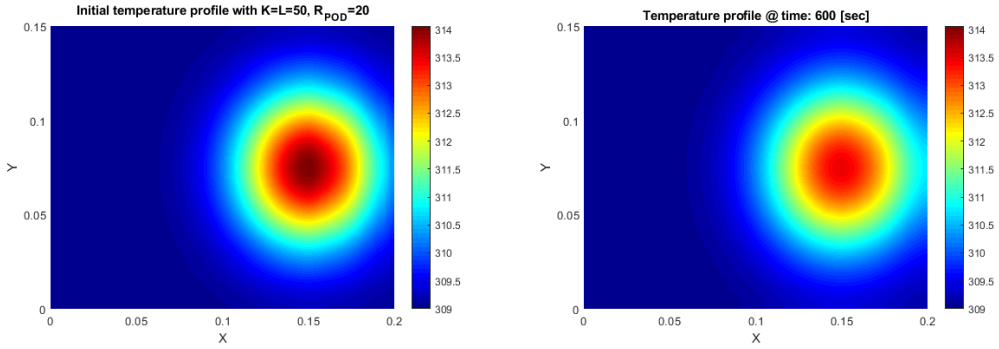

Figure 15 – POD basis initial profile over time with order R=20

Next the reduced order POD model is simulated with the same heat fluxes as during exercise 6 while varying R=3,20, as shown in Figure 16 and Figure 17 which are also almost identical.

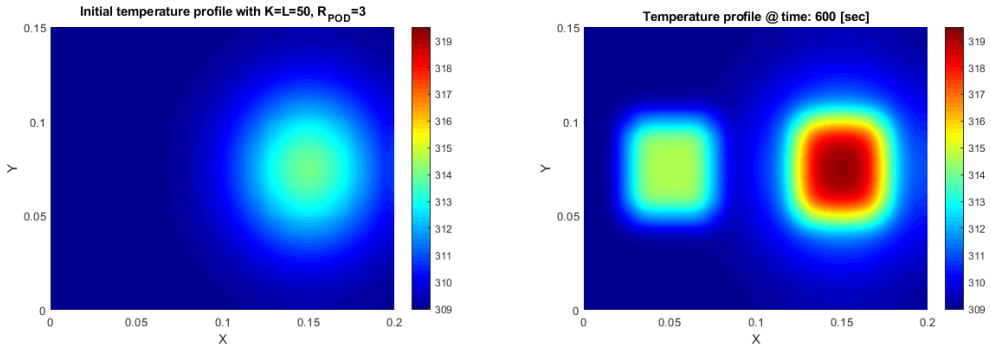

Figure 16 – POD basis initial temperature profile with inputs u1 and u2 over time with R=3

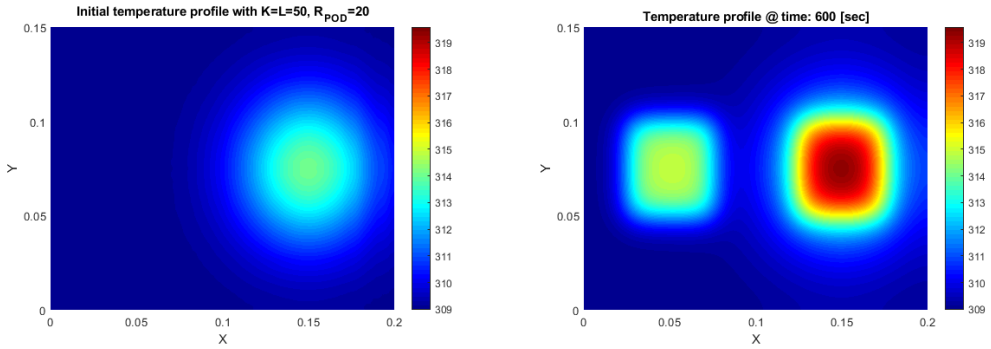

Figure 17 – POD basis initial temperature profile with inputs u1 and u2 over time with R=20

From the figures above can be concluded that the results are almost equal, indicating that a low POD order already has a high accuracy in comparison to the earlier determined basis when the initial temperature profile and input are the same.

Now the POD basis is simulated using a different initial temperature profile. The Bell curve is moved from the position of $u_2(t)$ to the position of $u_1(t)$ as shown in Figure 18 and Figure 19.

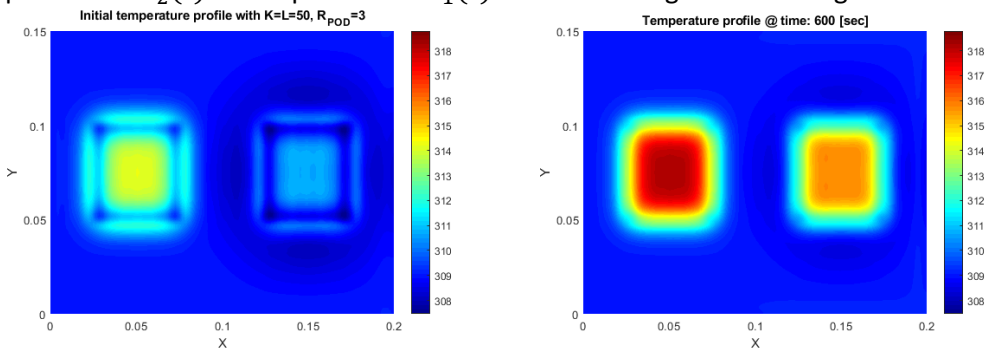

Figure 18 - POD basis adjusted initial profile over time with order R=3

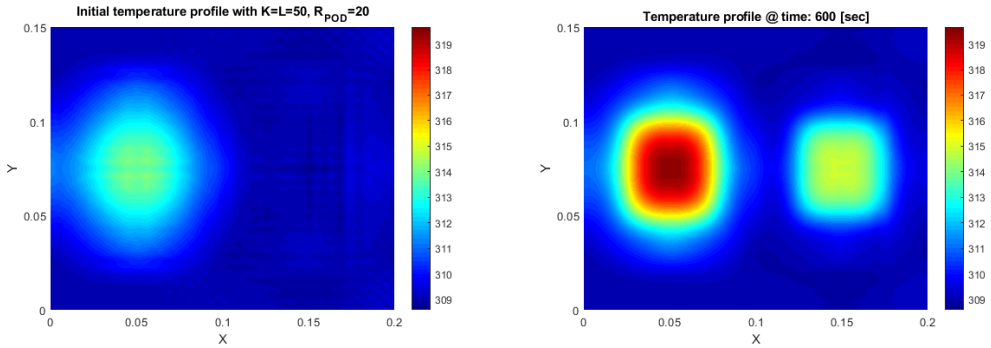

Figure 19 - POD basis adjusted initial profile over time with order R=20

Besides that, the input $u_1(t)$ and $u_2(t)$ are adjusted for the POD simulation by increasing the width of the square from 0.5 to 0.75 [m]. The results of these simulation are shown in Figure 20 and Figure 21.

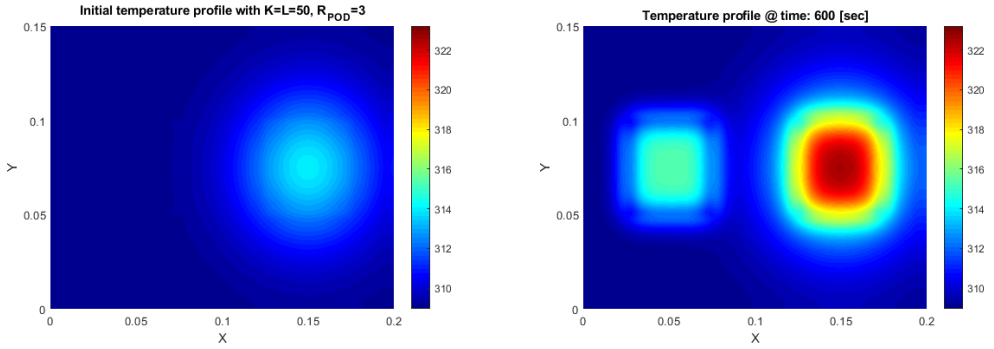

Figure 20 – POD basis initial temperature profile with adjusted inputs u1 and u2 over time with R=3

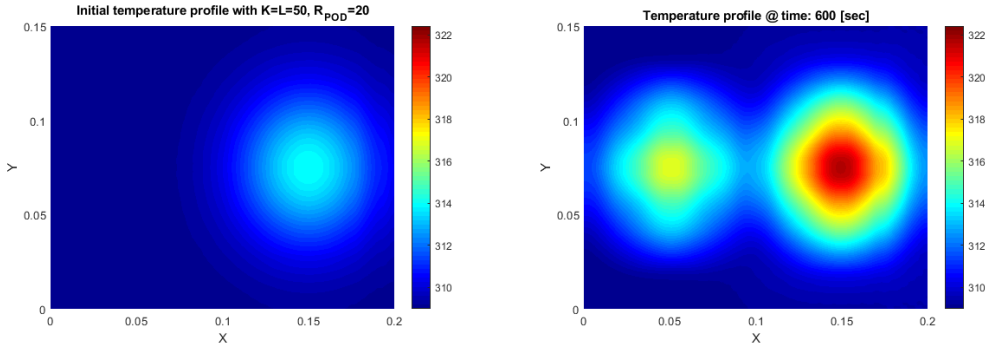

Figure 21 - POD basis initial temperature profile with adjusted inputs u1 and u2 over time with R=20

From these simulations can be concluded that a reduced order POD model only results in accurate estimations if the initial conditions and inputs are unchanged.

Exercise 10

For This exercise, a non-homogeneous material profile is considered in which a defined middle section has different ρ and c values. An ideal and approximated version of this material is visible in Figure 22.

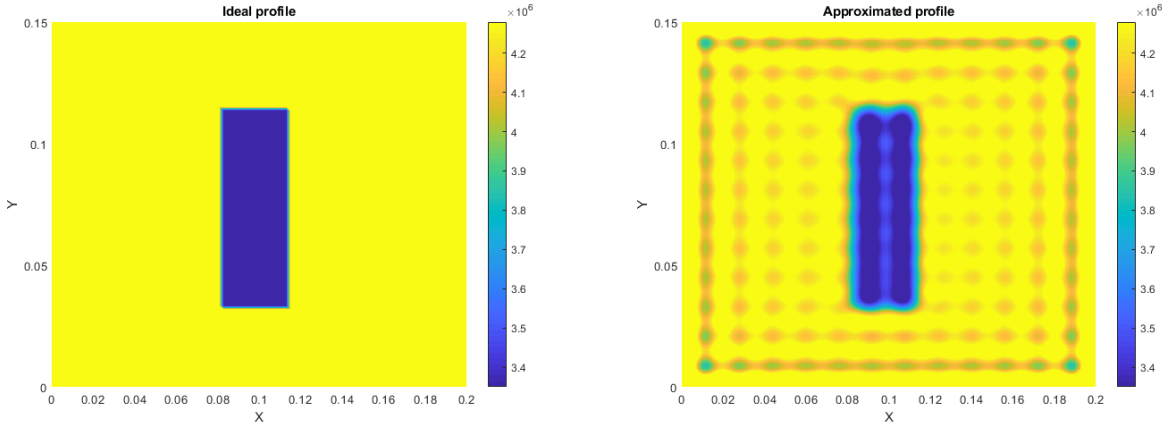

Figure 22 - non-homogeneous material profile

The approximation of this material profile is made using a Fourier expansion according to (39), with the same basis functions as used for the homogeneous model.

$$\rho(x,y)c(x,y) = \sum_{i=0}^{r} e_i \phi_i(x,y) \tag{39}$$

Now this approximation can be used to simulate the non-homogeneous model which can now be written as (40) and can be rewritten into equation (41).

$$\langle \sum_{i2=0}^{r} e_{i2}\phi_{i2} \sum_{i=0}^{r} \dot{a}_i\phi_i\,, \phi_j\rangle = \langle \kappa \sum_{i=0}^{r} a_i\ddot{\phi}_i^{(x)}\,, \phi_j\rangle + \langle \kappa \sum_{i=0}^{r} a_i\ddot{\phi}_i^{(y)}\,, \phi_j\rangle + \langle u, \phi_j\rangle \qquad (40)$$

$$\sum_{i=0}^{r} \dot{a}_i \sum_{i2=0}^{r} e_{i2}\langle \phi_{i2}\phi_i, \phi_j\rangle = \sum_{i=0}^{\infty} \kappa a_i \left(\langle \ddot{\phi}_i^{(x)}, \phi_j\rangle + \langle \ddot{\phi}_i^{(y)}, \phi_j\rangle\right) + \langle u, \phi_j\rangle \qquad (41)$$

This can now be used to simulate the non-homogeneous model in the same way as the homogeneous model, only instead of dividing the right side of the equation by the constant ρc, it is now multiplied with the inverse of the approximated $\rho(x,y)c(x,y)$ matrix. The result of the non-homogeneous model simulation is visible in Figure 23.

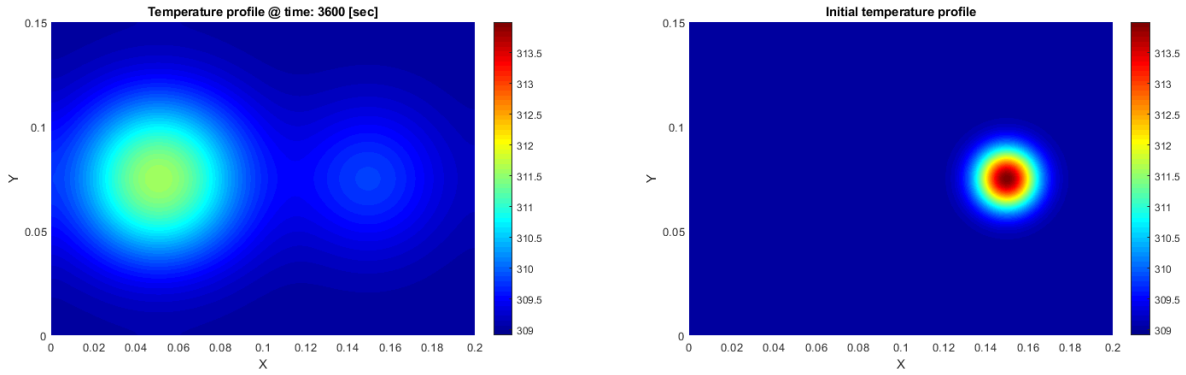

Figure 23 - non-homogeneous simulation

The difference with the homogeneous model is not clearly visible, the difference is that the heat does not conduct equally fast in all directions but a little faster towards the middle. The difference between the homogeneous and non-homogeneous model is better visible in the 1D case, as can be seen in Figure 24. Where the blue line represents the temperature of the non-homogeneous model and the red line the temperature of the homogeneous model.

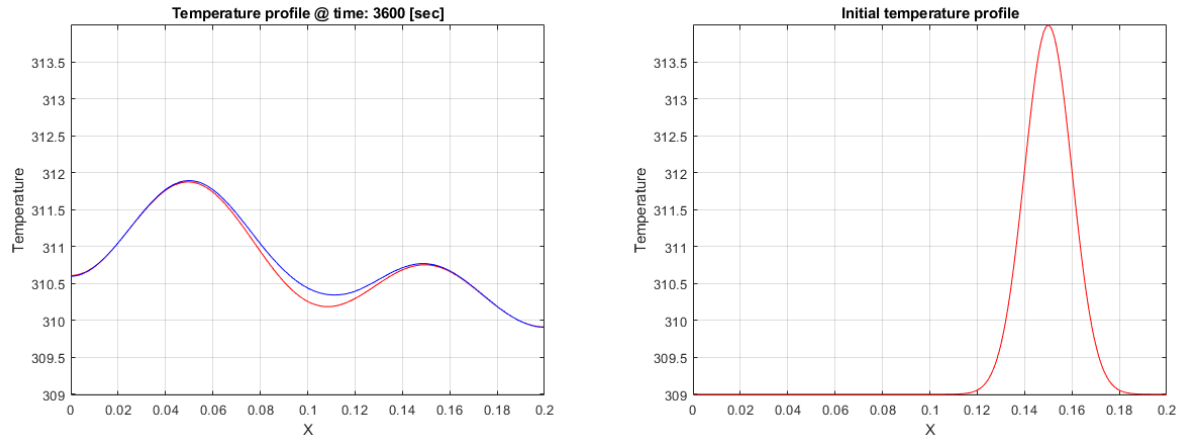

Figure 24 - non-homogeneous simulation 1D